

The effect of recombination and attachment on meteor radar diffusion coefficient profiles

C. S. Lee,^{1,2} J. P. Younger,^{2,3} I. M. Reid,^{2,3} Y. H. Kim,¹ and J. -H. Kim⁴

Received 29 August 2012; revised 3 March 2013; accepted 3 April 2013.

[1] Estimates of the ambipolar diffusion coefficient produced using meteor radar echo decay times display an increasing trend below 80–85 km, which is inconsistent with a diffusion-only theory of the evolution of meteor trails. Data from the 33 MHz meteor radar at King Sejong Station, Antarctica, have been compared with observations from the Aura Earth Observing System Microwave Limb Sounder satellite instrument. It has been found that the height at which the diffusion coefficient gradient reverses follows the height of a constant neutral atmospheric density surface. Numerical simulations of meteor trail diffusion including dissociative recombination with atmospheric ions and three-body attachment of free electrons to neutral molecules indicate that three-body attachment is responsible for the distortion of meteor radar diffusion coefficient profiles at heights below 90 km, including the gradient reversal below 80–85 km. Further investigation has revealed that meteor trails with low initial electron line density produce decay times more consistent with a diffusion-only model of meteor trail evolution.

Citation: Lee, C. S., J. P. Younger, I. M. Reid, Y. H. Kim, and J. -H. Kim (2013), The effect of recombination and attachment on meteor radar diffusion coefficient profiles, *J. Geophys. Res. Atmos.*, 118, doi:10.1002/jgrd.50315.

1. Introduction

[2] Estimates of the ambipolar diffusion coefficient in the atmosphere made using meteor radar echo decay times rely on the assumption that the development of meteor trails over time is governed only by diffusion. Comparisons of meteor radar diffusion coefficient estimates with independent measurements made by other types of sensors do not agree, which suggests that there is an additional mechanism affecting the meteor radar echo decay process. As diffusion coefficients are used to estimate temperatures near the mesopause, it is imperative to understand the source of this discrepancy.

[3] Meteoroids ablate following heating through collisions with atmospheric molecules and leave ionized trails in the height region around 70 to 110 km. Once a trail is formed, the ions and electrons diffuse away from the axis of a trail. This radial expansion of the trail leads to a decline in the observed intensity of radar backscatter over time. If the evolution of a trail is governed entirely by diffusive processes, then a meteor echo decays exponentially with time,

with a decay constant determined by the local ambipolar diffusion coefficient, as given by

$$D = 6.39 \times 10^{-2} \frac{T^2}{p} K_0, \quad (1)$$

where T is the atmospheric temperature, p is the pressure, and K_0 is the ionic mobility of the meteoric ions. A typical value for K_0 of $2.5 \times 10^{-4} \text{ m}^2 \text{ s}^{-1} \text{ V}^{-1}$ [Cervera and Reid, 2000] was used in this study, which corresponds to an olivine type meteor composition. The echo power of underdense meteor trails will decay exponentially over time due to diffusion, with a time taken to reach e^{-1} of the initial maximum value of

$$\tau = \frac{\lambda^2}{16\pi^2 D}, \quad (2)$$

where λ is the radar wavelength [McKinley, 1961]. Since the behavior of meteor echo decay is thought to be well described by ambipolar diffusion process within height range of 85–95 km, methods have been developed to use the decay time of meteor echoes to estimate temperatures near the mesopause region [Tsutsumi *et al.*, 1994; Hocking, 1999; Cervera and Reid, 2000; Kim *et al.*, 2012].

[4] According to equation (1), diffusion coefficients should increase with increasing height, due to the inverse proportionality of the diffusion coefficient with respect to atmospheric density. However, recent meteor radar observations, as in the examples shown in Figure 1, show that the estimate of the ambipolar diffusion coefficient increases with decreasing height below about 80 to 85 km [Ballinger *et al.*, 2008; Singer *et al.*, 2008; Younger *et al.*, 2008]. The increasing trend at lower heights is a significant discrepancy

¹Department of Astronomy and Space Science, Chungnam National University, Yuseong-gu, Daejeon, Republic of Korea.

²School of Chemistry and Physics, University of Adelaide, Adelaide, South Australia, Australia.

³ATRAD Pty. Ltd., Thebarton, South Australia, Australia.

⁴Korea Polar Research Institute, Yeonsu-gu, Incheon, Republic of Korea.

Corresponding author: J. P. Younger, School of Chemistry and Physics, University of Adelaide, Adelaide, SA, 5005, Australia. (joel.younger@adelaide.edu.au)

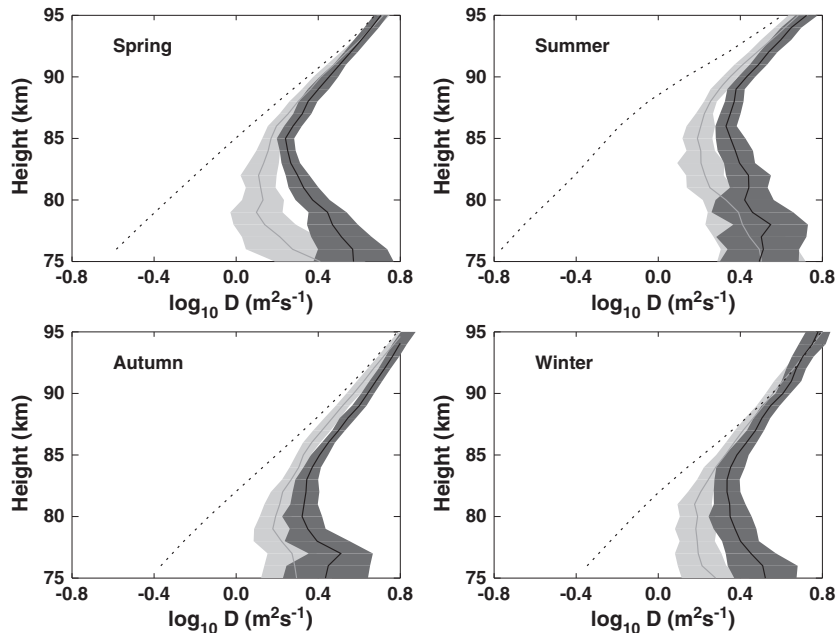


Figure 1. Height profiles of monthly mean diffusion coefficients for each season of 2012: 25% weakest meteor echoes in each height bin (light solid) and 25% strongest meteor echoes in each height bin (dark solid). Ambipolar diffusion coefficient profiles derived from Microwave Limb Sounder (MLS) data (dotted) are shown for comparison. The width of the shaded areas denotes one standard deviation.

in the behavior of meteor radar echo decay, as compared to the theoretical prediction of diffusion-only evolution. Furthermore, above 85 km, $\log D$ is approximately linear with respect to height, but the slope is less than what the values of T and p should dictate. This phenomenon is seen at all times of the year at all latitudes.

[5] In order to investigate the mechanism for the acceleration of meteor echo decay in the height region below 85 km, a comprehensive comparison between theory and observations is required. Previous work has restricted the modeling of meteor trail deionization to a single electron loss process [Baggaley, 1979]. Although several studies show that meteor radar diffusion coefficient estimates may be affected by electron removal by dust and icy particles [Havnes and Sigernes, 2005; Younger et al., 2008], low meteor detection rates have restricted the viability of diffusion coefficient profiles below 80 km. Aerosol models, however, do not produce the distinctive turnaround behavior seen at low altitudes at all times. Furthermore, aerosol models rely on very high attachment rates, which would most likely correspond to electron-scavenging ice crystals as seen in polar mesosphere summer echo and noctilucent cloud. As the low altitude turnaround effect is seen at all latitudes at all times of the year, it is probable that there is an additional mechanism affecting meteor radar echo decay times. Kim et al. [2010] explained the diffusion coefficient increase at low altitudes by constructing a simple model of electron loss due to ion-electron recombination. The authors demonstrated that diffusion coefficient turnaround occurs between 80 and 85 km in all seasons.

[6] In this study, we present a comparison of numerical simulations of the meteor radar diffusion coefficient height profiles with observations from a high-performance meteor

radar located at King Sejong Station, Antarctica. This represents the first study of its kind to consider the evolution of meteor radar echoes in the context of multiple chemical reactions. This will allow the dominant deionization mechanism responsible for the turnaround of the diffusion coefficient profile in the lower portion of the meteor detection region to be determined.

2. Observations

[7] To verify features of the meteor diffusion coefficient profile in the lower height region (below 80 km) in a statistically robust manner, high detection rate meteor data from 33 MHz radar at King Sejong Station, Antarctica (62.22°S, 58.78°W) was chosen for the study. This radar achieves typical detection rates of about 20,000–35,000 meteors per day, which includes sufficient data to extend the diffusion coefficient profile below 80 km without excessive uncertainty in the height-binned averages. The King Sejong radar uses a circularly polarized transmit antenna and a five-antenna receiving interferometer with ATRAD analysis software to optimize precise meteor detections. The analysis is identical to that used for the Buckland Park meteor radar, as described by Holdsworth et al. [2004], and applies a number of rejection criteria to reject echoes that do not exhibit under dense meteor characteristics. The operating parameters of the radar are summarized in Table 1.

[8] Satellite measurements of atmospheric temperature and density were used to determine the true diffusion coefficient height profile. The Aura satellite is in a 705 km high sun-synchronous orbit with an inclination of 98.2°. It carries EOS MLS (Earth Observing System Microwave Limb Sounder) instrument, a limb-scanning microwave emission

Table 1. Summary of Operating Parameters for the King Sejong Meteor Radar

Frequency (MHz)	33.2
Transmit power (kW)	12
Effective pulse width (km)	7.2
Pulse type	4 bit complementary
Pulse repetition frequency (Hz)	440
Duty cycle (%)	8.4
Coherent integrations	4
Range sampling resolution (km)	1.8
Effective sampling time (s)	0.009

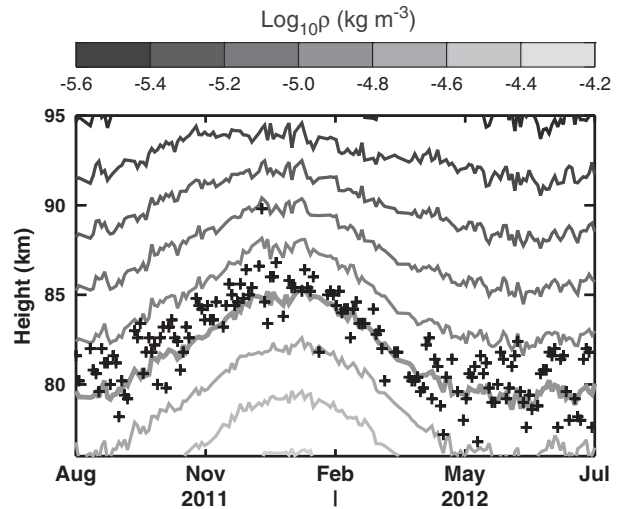
spectrometer composed of five radiometers operating across 118 GHz–2.5 THz to measure temperature and constituent densities on fixed pressure surfaces from the troposphere to the mesosphere. The MLS temperature and geopotential height are retrieved primarily from the band near O_2 spectral lines at 118 GHz on a fixed vertical pressure grid from 261 hPa to 0.001 hPa. MLS performs observations every 1.5° of arc in the direction of orbital motion by scanning the limb upward from the horizon [Schwartz *et al.*, 2008].

[9] To compare Aura EOS MLS data with radar measurements, MLS data within a 200 km radius of the meteor radar was used, corresponding to the primary meteor detection area of the radar. The MLS geopotential heights were converted to geometric altitudes using the WGS84 model and the hydrostatic relation in order to directly compare the satellite data with meteor radar observations.

[10] The meteor radar data used in this study were limited to zenith angles of less than 75° in order to avoid excessive uncertainties in the height estimate of distant meteors near the horizon. Detections were restricted to those above 75 km, in order to ensure there were sufficient detections present in the lowest bins of the diffusion coefficient profiles. Additionally, only meteors below 90 km were considered, in order to avoid possible geomagnetic effects [Jones, 1991; Dyrud *et al.*, 2001]. Above 95–100 km, the motion of ions and electrons becomes increasingly affected by the geomagnetic field, which would interfere with the assessment of electron loss mechanisms at low altitudes presented here.

[11] Diffusion coefficient height profiles were constructed by averaging meteor detection data in 1 km bins. To obtain monthly data of representative diffusion coefficient for both day and night, 6 h period meteor data was picked with local noon and midnight as the center, respectively. As D-region chemistry is the primary focus of this study with regard to the loss of electrons in the meteor trail, further analysis was restricted to daytime observations from both MLS and the meteor radar.

[12] A comparison of the diffusion coefficient turnaround height with atmospheric densities derived from MLS data indicates that turnaround height is determined by atmospheric density. A second-order polynomial fit was applied to the 2 day averaged height profile of diffusion coefficient estimates, and the turnaround height was defined as the inflection point of the fitted curve. Figure 2 shows atmospheric neutral density derived from MLS and turnaround height of diffusion coefficient estimates from the King Sejong Station meteor radar from August 2011 to July 2012. It should be noted that diffusion coefficient profile turnaround occurs at a fixed atmospheric density regardless

**Figure 2.** Heights of constant density surfaces of the neutral atmosphere from Aura EOS MLS (contours) and height of meteor radar diffusion coefficient turnaround (crosses) for daytime observations at King Sejong Station, Antarctica, from August 2011 through July 2012.

of the season. In general, neutral temperature can change the rates of electron removal processes, such as recombination and attachment, but observations showed no correlation between atmospheric temperature and meteor radar diffusion coefficient turnaround height. Hence, it appears that the neutral atmospheric density is the dominant term controlling the turnaround of meteor radar diffusion coefficients at low altitudes.

3. Meteor Trail Chemistry

[13] The reactions that affect meteoric plasma are summarized in Table 2. The lower portion of the region where meteor trails form corresponds to the upper region of the D-layer of the ionosphere, and thus background ions must be included to fully describe the development of meteoric plasma. Additionally, background neutral molecules can absorb free electrons from the meteor trail.

[14] The positive ions in the upper D-region above 80 km are primarily NO^+ and O_2^+ [Nicolet and Aikin, 1960], which remove free electrons from meteor trails by dissociative recombination. NO^+ and O_2^+ are mostly produced through photoionization, with much smaller quantities produced by the interaction of ionized atomic oxygen from the meteor trail with neutral N_2 and O_2 from the background atmosphere [Baggaley, 1979]. Thus, any effect on meteor trail evolution due to dissociative recombination with NO^+ and O_2^+ should exhibit a strong temporal dependence following the level of insolation.

[15] In situ measurements have reported that there is a transition around 80 km where the dominant positive ions switches from NO^+ , O_2^+ to water cluster ions of the form $H^+(H_2O)_n$ [Narcisi *et al.*, 1972; Kopp and Herrmann, 1984], where n is the number of water molecules in the cluster. The reaction rate for the dissociative recombination of electrons with water cluster ions exceeds that of NO^+ and O_2^+ by at

Table 2. Chemical Processes and Reaction Rates Used in Numerical Simulation of Meteor Trail Evolution

Reaction Process	Rate Coeff.	Reaction Rate	Rate Source	Reaction Type
$O^+ + O_2 \rightarrow O_2^+ + O$	k_1	$2.5 \times 10^{-17} \text{ m}^3 \text{ s}^{-1}$	<i>Lindinger et al.</i> [1974]	Charge
$O^+ + N_2 \rightarrow NO^+ + N$	k_2	$2.0 \times 10^{-18} \text{ m}^3 \text{ s}^{-1}$	<i>Lindinger et al.</i> [1974]	Transfer
$O_2^+ + e^- \rightarrow O + O$	k_3	$2.2 \times 10^{-13} \text{ m}^3 \text{ s}^{-1}$	<i>Walls and Dunn</i> [1974]	Dissociative Recombination
$NO^+ + e^- \rightarrow N + O$	k_4	$7.0 \times 10^{-13} \text{ m}^3 \text{ s}^{-1}$	<i>Walls and Dunn</i> [1974]	
$H^+(H_2O)_n + e^- \rightarrow H(H_2O)_{n-1} + H_2O$	k_5	$3.0 \times 10^{-12} \text{ m}^3 \text{ s}^{-1}$	<i>Reid</i> [1977]	Cluster ion recombination
$O_2 + e^- + O_2 \rightarrow O_2 + O_2$	k_6	$3.8 \times 10^{-42} \text{ m}^6 \text{ s}^{-1}$	<i>McCorkle et al.</i> [1972]	Three-body
$O_2 + e^- + N_2 \rightarrow O_2 + N_2$	k_7	$1.5 \times 10^{-43} \text{ m}^6 \text{ s}^{-1}$	<i>McCorkle et al.</i> [1972]	Attachment

least an order of magnitude [Reid, 1977]. Therefore, the loss of electrons through dissociative recombination with water cluster ions can be the most significant recombinative process below 80 km, depending on the seasonal concentration of water cluster ions in the mesosphere [Reid, 1970].

[16] The loss of free electrons from meteor trails due to the attachment of electrons to neutral atmospheric molecules, in the form of three-body attachment, has significant potential to alter the evolution of meteoric plasma [Baggaley and Cummack, 1974; Rodriguez and Inan, 1994]. Although several laboratory measurements [e.g., Chanin et al., 1959] of three-body attachment coefficient have been made, it is uncertain whether these values can be applied at the atmospheric pressures, electron energies and with the constituents appropriate to meteor trails [Greenhow and Hall, 1961]. Despite the uncertainty in the precise value of the three-body attachment coefficient, the exponential increase in the density of atmospheric molecules with decreasing height should produce a corresponding increase in the rate of electron attachment. Thus, low altitude meteors should see significant numbers of free electrons lost due to three-body attachment processes.

4. Numerical Simulation Method

[17] The reactions summarized in Table 2 can be included in the diffusion equations for each species to model the development of meteor trail plasma in a reactive environment. Metal ions produced by the meteor generally recombine at very slow rates, as compared to other processes, so recombination with metal ions can be ignored [Baggaley, 1979]. The diffusion-only development of the metal ion distribution is then given by

$$\frac{\partial}{\partial t}[M^+] = D\nabla^2[M^+]. \quad (3)$$

[18] Ionized atomic oxygen may constitute as much as 75% of the positive ions in meteor trails, due to the ionization of oxygen liberated from the meteor during ablation and the ionization of atmospheric oxygen during collisions with prethermalized meteoric debris. The ionized atomic oxygen in the trail diffuses outward from the trail axis and is destroyed through charge transfer processes with neutral N_2 and O_2 from the background atmosphere, as given by

$$\frac{\partial}{\partial t}[O^+] = D\nabla^2[O^+] - k_1[O^+][O_2] - k_2[O^+][N_2]. \quad (4)$$

[19] O_2^+ and NO^+ are present in the atmosphere due to photoionization and are produced in the trail through the process of charge transfer between O^+ and neutral atmospheric molecules. The evolution of the populations of these species is governed by the following equations:

$$\frac{\partial}{\partial t}[O_2^+] = D\nabla^2[O_2^+] + k_1[O^+][O_2] - k_3[O_2^+][e^-] \quad (5)$$

and

$$\begin{aligned} \frac{\partial}{\partial t}[NO^+] = & D\nabla^2[NO^+] + k_2[O^+][N_2] \\ & - k_4[NO^+][e^-]. \end{aligned} \quad (6)$$

[20] Water cluster ions present a significant sink for free electrons, provided they are present in sufficient quantities. The absorption of free electrons by water cluster ions is much faster than other recombinative processes; with diffusion, the change in number density is given by

$$\begin{aligned} \frac{\partial}{\partial t}[H^+(H_2O)_n] = & D\nabla^2[H^+(H_2O)_n] \\ & - k_5[H^+(H_2O)_n][e^-]. \end{aligned} \quad (7)$$

[21] The free electrons in a meteor trail scatter radio waves for detection by radar and are of primary interest in the modeling of meteor trails. Combining diffusion with the electron loss reactions from Table 2, the development of free electrons in the meteor trail is given by

$$\begin{aligned} \frac{\partial}{\partial t}[e^-] = & D\nabla^2[e^-] - k_3[O_2^+][e^-] - k_4[NO^+][e^-] \\ & - k_5[H^+(H_2O)_n][e^-] - k_6[O_2]^2[e^-] \\ & - k_7[O_2][N_2][e^-]. \end{aligned} \quad (8)$$

The densities of O_2 and N_2 at each height were left static, as the densities of neutral molecules are much larger than those of any positive ion species or that of the free electrons in underdense meteor trails.

[22] The densities of ions for dissociative recombination were held constant at all heights at higher typical values of 10^{10} m^{-3} , as derived from daytime rocket measurements [Reid, 1970; Kopp and Herrmann, 1984] and the International Reference Ionosphere 2012. Although this probably represents an overestimation of the true densities of O_2^+ , NO^+ below 80 km and for water cluster ions above, the difference is negligible in the total density of ions. The aggressive choice of NO^+ and O_2^+ ion densities at lower altitudes provides an opportunity to determine if dissociative recombination could play a meaningful role in the

development of the turnaround phenomenon. An alternate distribution of water cluster ions was also used to determine if high cluster ion densities at low altitude could be responsible for turnaround.

[23] The supplied values of density and the ambipolar diffusion coefficient were obtained from Aura EOS MLS data for King Sejong Station, Antarctica. Profiles representative of summer and winter conditions were used to assess the seasonal variability of the predictions.

[24] Equations (3) through (8) were solved simultaneously using a fourth-order Runge-Kutta method. The radius of the Gaussian initial distribution of the meteor trail was calculated as $r_0 = 0.0028\rho^{-0.25}v^{0.6}$, where ρ is the atmospheric density [Ceplecha et al., 1998]. The velocity of the meteor, v , was set to 35 km s^{-1} , which corresponds to the peak of the sporadic meteor velocity distribution. The spatial basis at each height level of the simulation was constructed from 250 bins at a spacing of $r_0/25$. An adaptive time step was used to ensure that the relative change in all quantities at each point in space remained below 1% at all times. A maximum time step of 1 ms was also used.

[25] The radial diffusion and reactions between the constituents of the trail was then calculated over a range of diffusion coefficients and initial electron line densities. Supplied values of the initial electron line density ranged from 10^{13} to 10^{14} m^{-1} , which corresponds to typical line densities of underdense meteors detected by meteor radars. The amplitude of the backscattered radio signal from the trail was calculated at each time step using the equation

$$A \propto 2\pi \int_0^\infty [e^-] r J_0 \left(\frac{4\pi r}{\lambda} \right) dr \quad (9)$$

[26] The decay time, τ , for a meteor trail with each combination of parameters was determined by the time taken for the condition $A(t)/A(0) = \exp(-1)$ to be satisfied. The predicted value of decay time was then converted to a diffusion coefficient using equation 2.

[27] The predicted value of the diffusion coefficient estimate was then compared with the input value of the diffusion coefficient to determine the effect of different reactions in the trail. By using different values of the diffusion coefficient and atmospheric density, predicted diffusion coefficient estimate height profiles were constructed for different atmospheric conditions. The inclusion of Aura MLS data allowed direct comparison of the predicted diffusion coefficient profiles with meteor radar observations, using real values of ρ and D in the model.

5. Model Predictions

[28] Under all conditions, the model predictions indicate that the loss of electrons to three-body attachment is the dominant mechanism responsible for the distortion of meteor diffusion coefficient profiles inferred from meteor radar echo decay times. The effect of three-body attachment can be summarized by three effects on the observed height profile of diffusion coefficient estimates, which can be seen in Figure 3. The loss of electrons to three-body attachment reduces the decay time, causing an overestimation of the ambipolar diffusion coefficient at all heights. This offset increases with decreasing height, causing the slope of the approximately linear portion of $\log D$ above about 85 km to

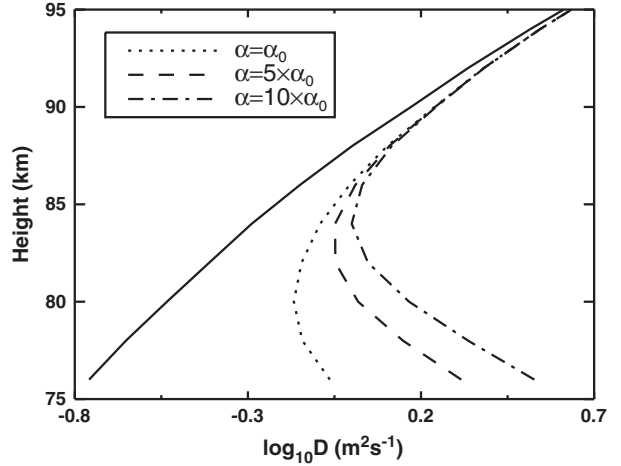


Figure 3. Numerical simulation of height profiles of diffusion coefficient estimates for different multiples of the original three-body attachment rate (broken lines) compared with the true input value of the diffusion coefficient (solid line).

differ from the slope of the logarithm of the true ambipolar diffusion coefficient. Finally, between about 80–85 km, the loss of electrons to three-body attachment has such a sufficient effect that the slope of $\log D$ reverses and the diffusion coefficient increases with decreasing altitude.

[29] It was found that the turnaround height is sensitive to the value of the three-body attachment coefficient. Using the values shown in Table 2, the diffusion coefficient turnaround occurred at lower altitudes than was seen in observations. If the attachment rates were increased by a factor of 2.5, then the predicted turnaround behavior became consistent with observations, as seen in the overlaid simulated profiles in Figure 4.

[30] Although Greenhow and Hall [1961] only used long duration meteor trails to explain the rapid disappearance of free electrons at heights near 80 km with three-body attachment, they also provide an insight into the process responsible for diffusion of meteor trails other than ambipolar diffusion. As the atmospheric density increase with decreasing height, the reduction rate of electron loss via three-body attachment increases in proportion to the square of atmospheric density. The model predicts that the loss of electrons in meteor trail below around 85 km is dominated by three-body attachment to neutral background molecules, as seen in Figure 4. Thus, this mechanism is responsible for the turnaround behavior at low heights.

[31] Baggaley [1979] reported that dissociative recombination plays a significant role in the removal of electrons from meteor trails with high initial electron line densities. However, the model predicted that this chemical reaction has a negligible effect on the diffusion coefficient turnaround phenomenon. When the model only used the dissociative recombination as a sink for electrons, the predicted features of diffusion coefficient estimate profile were nearly identical with that of the input diffusion coefficient profile, regardless of electron line density.

[32] Similarly, the loss of electrons to dissociative recombination with water cluster ions did not have an appreciable

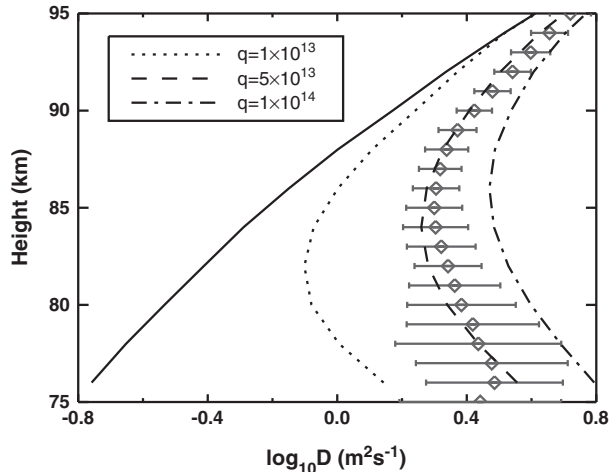


Figure 4. Observed daytime diffusion coefficient profile for January 2012 at King Sejong Station, Antarctica, taken from Aura EOS MLS satellite instrument (solid line) and the 33 MHz meteor radar (error bars). Numerical simulations for different initial electron line densities are shown for comparison (broken lines).

effect on the shape of the diffusion coefficient profile. The extreme case of water cluster ion density being proportional to atmospheric density was considered, with a maximum value of 10^{10} m^{-3} at 75 km. Even with this exaggerated density profile, there was no discernible change to the diffusion coefficient profile.

[33] The model predicted that meteor trails with different initial electron line densities will experience different degrees of electron loss, relative to the initial electron density. The relative electron line densities of different meteor trails can be inferred from the meteor radar response function [Cepilecha *et al.*, 1998], which provides the attenuation due to range, R , at a given wavelength to be a factor of $(R/\lambda)^{3/2}$. Thus, the relative electron line density of the trail, uncalibrated for receiver gain is given by $q \propto (P_R R^3 \lambda^{-3})^{1/2}$, where P_R is the received echo power.

[34] This relation was used to calculate the uncalibrated electron line densities of meteor detections in each height bin of each profile, which were then divided into the weakest and strongest quartiles for comparison. Meteor trails with low initial electron line densities, which corresponds to the detection quartile of low range-adjusted echo strength, produce decay times more consistent with diffusion-only trail evolution, as seen in the studies by Baggaley [1979] and Kim *et al.* [2010]. The deviation between the predicted value of the diffusion coefficient estimate and the input diffusion coefficient value increases at lower heights and higher electron densities. As a result, meteor trails with higher electron density undergo diffusion coefficient turnaround at higher altitudes.

[35] This contradicts the findings of Havnes and Sigernes [2005] and Younger *et al.* [2008] that predict that stronger echoes should produce better agreement with the ambipolar diffusion coefficient. Those models, however, are concerned with the absorption of free electrons by aerosols. Furthermore, while aerosols will absorb free electrons at low altitudes, such a model requires high values of the

attachment rate and aerosol density that are not present at all altitudes in all seasons. The required high values of the attachment rate and aerosol density are only even plausible in the presence of polar mesospheric clouds. Given that low altitude turnaround occurs and behaves consistently in all seasons, it is unlikely that aerosol attachment plays a strong role. Additionally, meteor mass injection drops significantly below 85 km [Plane, 2012], making the already electron loss rate to small ($< 5 \text{ nm}$) meteoric smoke particles with small attachment rates negligible. While aerosol attachment certainly does play some role in the modification of meteor radar echo decay times, limitations on aerosol density and attachment rates, as well as seasonal and latitudinal variations make three-body attachment a better candidate for the source mechanism of the low-altitude turnaround effect.

[36] As shown in Figure 2, the turnaround height of the meteor radar diffusion coefficient profile closely follows the height of an atmospheric constant density surface. The predicted diffusion coefficient height profiles from the model displayed similar differences between summer and winter conditions both on turnaround height and on the gradient of $\log D$ due to the significant seasonal variation in atmospheric density and density scale height.

6. Conclusions

[37] This study has examined, for the first time, the diffusion of meteor trails including the reactions between atmospheric ions, ionized atomic oxygen in the meteor trail, and free electrons. The results of numerical simulations are consistent with the observations of a gradient reversal of the meteor radar diffusion coefficient profile below 80–85 km. This indicates that the decay times of meteor radar echoes at lower altitudes are significantly affected by deionization processes that can dominate the development of the meteor radar echoes over the effects of radial diffusion.

[38] The model predicted that the turnaround of the diffusion coefficient profile occurs at all times and is a function of the background neutral density and the initial electron line density of the trail. A comparison of the turnaround height of meteor radar diffusion coefficient profiles with data from the Aura EOS MLS instrument displayed the same behavior.

[39] A detailed examination of the different processes included in the numerical model indicates that three-body attachment of meteor trail electrons to neutral atmospheric molecules is responsible for the deionization of meteor trails at low altitudes and the attendant turnaround of the diffusion coefficient profile. Dissociative recombination, whether with NO^+ , O_2^+ , or water cluster ions, does not have a significant effect on the decay time of meteor radar echoes. It was further found that the decay times of weak echoes with low initial electron line densities are significantly less affected by the removal of free electrons from the trail.

[40] In this study, the three-body attachment coefficient was required to be at least 2.5 times larger than the published values in order to precisely duplicate the observed structure of the meteor radar diffusion coefficient profile. It is therefore important to establish a better understanding of the factors that determine the rate at which three-body attachment occurs.

[41] The removal of electrons through three-body attachment has three significant effects on the height profile of diffusion coefficient estimates inferred from meteor radar echo decay times. At all heights, the removal of free electrons from meteor trails reduces the decay times of radar echoes, leading to an increase in the diffusion coefficient estimate. The severity of this effect increases with decreasing altitude, causing the slope of the estimate of $\log D$ with respect to height to be smaller than the slope of the true value of $\log D$. At a height between 80 and 85 km, the slope of $\log D$ reverses completely, causing D to increase with decreasing height. In light of these findings, meteor echoes from trails with low initial electron line density will provide more reliable estimates of the ambipolar diffusion coefficient. Furthermore, the reduction of meteor radar echo decay times due to three-body attachment may degrade the accuracy of temperatures obtained from meteor radar decay times below 90 km, unless a method to correct for the effects of deionization is introduced.

[42] **Acknowledgments.** This study has been supported in part by the National Research Foundation of Korea grant funded by the Korea government (MEST) and also by Korea Polar Research Institute (PE12010). Additional funding was provided by Australian Research Council grant DP1096901. Helpful comments and continuous support from Space and Atmospheric Physics Group in University of Adelaide are appreciated.

References

- Baggaley, W. J., and C. H. Cummack (1974), Meteor train ion chemistry, *J. Atmos. Terr. Phys.*, *36*, 1759–1773.
- Baggaley, W. J. (1979), The influence of recombination on under-dense radio-meteor data, *Plan. Space Sci.*, *27*, 905–907.
- Ballinger, A. P., P. B. Chilson, R. D. Palmer, and N. J. Mitchell (2008), On the validity of the ambipolar diffusion assumption in the polar mesopause region, *Ann. Geophys.*, *26*(1), 3439–3443.
- Cepelcha, Z., J. Borovička, W. G. Elford, D. O. ReVelle, R. L. Hawkes, V. Porubčan, and M. Šimek (1998), Meteor phenomena and bodies, *Space Sci. Rev.*, *84*, 327–471.
- Cervera, M. A., and I. M. Reid (2000), Comparison of atmospheric parameters derived from meteor observations with CIRA, *Radio Sci.*, *35*(3), 833–843.
- Chanin, L. M., A. V. Phelps, and M. A. Biondi (1959), Measurement of the attachment of slow electrons in oxygen, *Phys. Rev. Lett.*, *2*(8), 344–346.
- Dyrud, L., M. Oppenheim, and A. vom Endt (2001), The anomalous diffusion of meteor trails, *Geophys. Res. Lett.*, *28*(14), 2775–2778.
- Greenhow, J. S., and J. E. Hall (1961), Attachment processes in meteor trails, *J. Atmos. Terr. Phys.*, *21*, 261–271.
- Havnes, O., and F. Sigernes (2005), On the influence of background dust on radar scattering from meteor trails, *J. Atmos. Sol-Terr. Phys.*, *67*, 659–664.
- Hocking, W. K. (1999), Temperatures using radar-meteor decay times, *Geophys. Res. Lett.*, *26*(21), 3297–3300.
- Holdsworth, D. A., I. M. Reid, and M. A. Cervera (2004), Buckland Park all-sky interferometric meteor radar, *Radio Sci.*, *39*(5), RS5009.
- Jones, W. (1991), Theory of diffusion of meteor trains in the geomagnetic field, *Plan. Space Sci.*, *39*(9), 1283–1288.
- Kim, J.-H., Y. H. Kim, C. S. Lee, and G. Jee (2010), Seasonal variation of meteor decay times observed at King Sejong Station (62.22°S, 58.78°W), Antarctica, *J. Atmos. Sol-Terr. Phys.*, *72*, 883–889.
- Kim, J.-H., Y. H. Kim, G. Jee, and C. S. Lee (2012), Mesospheric temperature estimation from meteor decay times of weak and strong meteor trails, *J. Atmos. Sol-Terr. Phys.*, *89*, 18–26.
- Kopp, E., and U. Herrmann (1984), Ion composition in the lower ionosphere, *Ann. Geophys.*, *2*(1), 83–94.
- Lindinger, W., F. C. Fehsenfeld, A. L. Schmeltekopf, and E. E. Ferguson (1974), Temperature dependence of some ionospheric ion-neutral reactions from 300–900 K, *J. Geophys. Res.*, *79*(31), 4753–4756.
- McCorkle, D. L., L. G. Christophorou, and V. E. Anderson (1972), Low energy (1 eV) electron attachment to molecules at very high gas densities: O₂, *J. Phys. B: Atom. Molec. Phys.*, *5*, 1211–1220.
- McKinley, D. W. R. (1961), *Meteor Science and Engineering*, McGraw-Hill, New York.
- Narcisi, R. S., A. D. Baily, L. E. Wlodyka, and C. R. Philbrick (1972), Ion composition measurements in the lower ionosphere during the November 1966 and March 1970 solar eclipses, *J. Atmos. Terr. Phys.*, *34*, 647–658.
- Nicolet, M., and A. C. Aikin (1960), The formation of the D region of the ionosphere, *J. Geophys. Res.*, *65*(5), 1469–1483.
- Plane, J. (2012), Cosmic dust in the Earth's atmosphere, *Chem. Soc. Rev.*, *41*(19), 6507–6518.
- Reid, G. C. (1970), Production and loss of electrons in the quiet daytime D region of the ionosphere, *J. Geophys. Res.*, *75*(13), 2551–2562.
- Reid, G. C. (1977), The production of water-cluster positive ions in the quiet daytime D region, *Plan. Space Sci.*, *25*, 275–290.
- Rodriguez, J. V., and U. S. Inan (1994), Electron density changes in the nighttime D region due to heating by very-low-frequency transmitters, *Geophys. Res. Lett.*, *21*(2), 93–96.
- Schwartz, M. J., et al. (2008), Validation of the aura microwave limb sounder temperature and geopotential height measurements, *J. Geophys. Res.*, *113*, D15S11.
- Singer, W., R. Latteck, L. F. Millan, N. J. Mitchell, and J. Fiedler (2008), Radar backscatter from underdense meteors and diffusion rates, *Earth Moon Planets*, *102*, 403–409.
- Tsutsumi, M., T. Tsuda, T. Nakamura, and S. Fukao (1994), Temperature fluctuations near the mesopause inferred from meteor observations with the middle and upper atmosphere radar, *Radio Sci.*, *29*(3), 599–610.
- Walls, F. L., and G. H. Dunn (1974), Measurement of total cross sections for electron recombination with NO⁺ and O₂⁺ using ion storage techniques, *J. Geophys. Res.*, *79*(13), 1911–1915.
- Younger, J. P., I. M. Reid, R. A. Vincent, and D. A. Holdsworth (2008), Modeling and observing the effect of aerosols on meteor radar measurements of the atmosphere, *Geophys. Res. Lett.*, *35*, L15812.